Parametric amplification by coupled flux qubits

M. Rehák, P. Neilinger, M. Grajcar, G. Oelsner, U. Hübner, E. Il'ichev, and H.-G. Meyer

Citation: Applied Physics Letters **104**, 162604 (2014); doi: 10.1063/1.4873719
View online: http://dx.doi.org/10.1063/1.4873719
View Table of Contents: http://scitation.aip.org/content/aip/journal/apl/104/16?ver=pdfcov
Published by the AIP Publishing

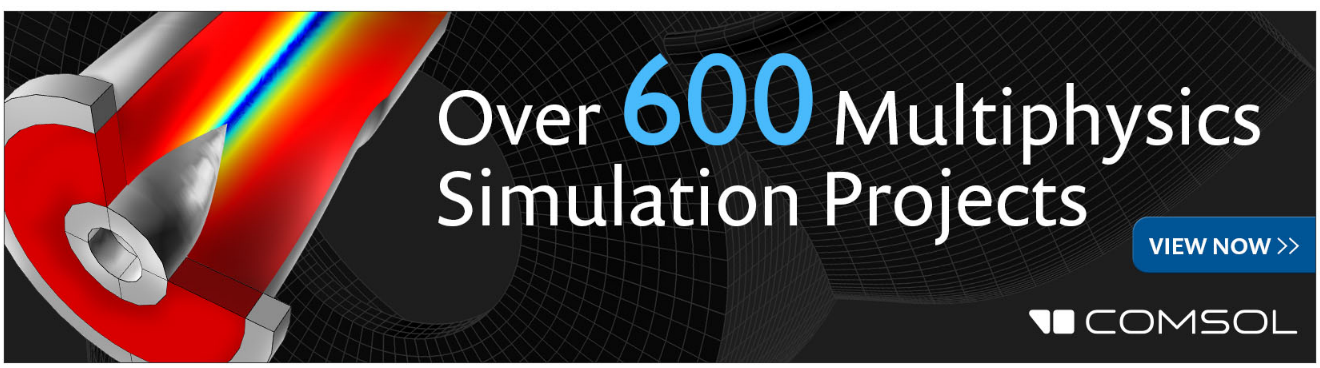

APPLIED PHYSICS LETTERS **104**, 162604 (2014)

Parametric amplification by coupled flux qubits

M. Rehák,[1,2] P. Neilinger,[1,2] M. Grajcar,[1,2] G. Oelsner,[3] U. Hübner,[3] E. Il'ichev,[3,4] and H.-G. Meyer[3]
[1]*Department of Experimental Physics, Comenius University, SK-84248 Bratislava, Slovakia*
[2]*Institute of Physics, Slovak Academy of Science, 845 11 Bratislava, Slovakia*
[3]*Leibniz Institute of Photonic Technology, P.O. Box 100239, D-07702 Jena, Germany*
[4]*Novosibirsk State Technical University, 20 K. Marx Ave., 630092 Novosibirsk, Russia*

(Received 27 December 2013; accepted 17 April 2014; published online 25 April 2014)

We report parametric amplification of a microwave signal in a Kerr medium formed from superconducting qubits. Two mutually coupled flux qubits, embedded in the current antinode of a superconducting coplanar waveguide resonator, are used as a nonlinear element. Shared Josephson junctions provide the qubit-resonator coupling, resulting in a device with a tunable Kerr constant (up to 3×10^{-3}) and a measured gain of about 20 dB. This arrangement represents a unit cell which can be straightforwardly extended to a quasi one-dimensional quantum metamaterial with large tunable Kerr nonlinearity, providing a basis for implementation of wide-band travelling wave parametric amplifiers. © *2014 AIP Publishing LLC*. [http://dx.doi.org/10.1063/1.4873719]

Recent development in circuit quantum electrodynamics has resulted in the possibility of signal detection close to and even below the standard quantum limit. This work was motivated by microwave quantum engineering,[1–3] including quantum information processing devices.[4,5] The sensitivity of cryogenic semiconductor amplifiers with reasonable power consumption in both the MHz[6] and GHz (commercially available) range are all currently above the quantum limit. The noise temperature of cryogenic high-electron-mobility transistor (HEMT) amplifiers in the GHz range is above 1 K. At very low temperatures below 1 K, it is quite natural to use the parametric effect for amplification which adds no additional noise to the signal. In practice, a nonlinear superconducting oscillator can be used for this purpose.[7,8] There, usually the nonlinearity of superconducting weak links[9,10] is exploited. Very recently squeezing of quantum noise and its measurement below the standard quantum limit was demonstrated.[11] These experiments have motivated the development of new parametric amplifiers based on Josephson junctions,[12,13] Superconducting Quantum Interference Devices (SQUID),[13–15] the high kinetic inductance of weak links,[16] or disordered superconductors.[17] Superconducting qubits also exhibit a strong nonlinearity[18] and therefore are good candidates for parametric amplification.[19]

In this paper, we demonstrate parametric amplification exploiting the nonlinearity of a pair of superconducting flux qubits coupled to a coplanar waveguide resonator. Here, our goal is two-fold: to demonstrate the parametric amplification with a two-qubit system, exhibiting potentially large Kerr constant, and to compare the obtained results with existing theoretical models.

The interaction of standing waves with a nonlinear medium in a resonator leads to nonlinear oscillations. Neglecting the interactions between the modes, the Hamiltonian of such an oscillator can be written as[20]

$$H_n = \hbar\omega_n a^\dagger a + \frac{\hbar}{2} K_n a^\dagger a^\dagger a a, \tag{1}$$

where $\hbar$ is the reduced Planck constant, a and $a^\dagger$ are the creation and the annihilation operators, respectively, ω_n is the angular frequency of the n-th mode of the oscillator, and K_n is the Kerr constant, which is a measure of the nonlinearity in the system. For our practical realization, the qubits contribute to the nonlinear inductance of the resonator per unit length according to

$$\tilde{L}_r(I_r) = \tilde{L}_0 + \tilde{L}_2(I_r/I_{cqr})^2 + \tilde{L}_4(I_r/I_{cqr})^4 + \ldots. \tag{2}$$

Then, the Kerr constant can be calculated by[20]

$$K_n = -\frac{\hbar\omega_n^2}{I_{cqr}^2}\int_0^l dx u_n^4(x)\tilde{L}_2, \tag{3}$$

where $u_n(x) = \sqrt{\frac{2}{\tilde{L}_r l}}\sin(\frac{n\pi x}{l})$, l is the length of the resonator, $\tilde{L}_r$ is the linear inductance of the resonator per unit length, I_r is the current in the resonator, I_{cqr} is the critical current of the Josephson junction shared by the resonator and the qubit, and $\tilde{L}_i$ are the Taylor coefficients characterizing the nonlinearity of the inductance.

The Kerr constant can be determined for every nonlinear medium. In optics, the Kerr constants are very small, while wide-band travelling wave amplifiers require large ones. Even for a single superconducting qubit the Kerr constant is not small. It may be further enhanced by using ferromagnetically coupled qubits.[21,22] A pair of qubits can be considered as a unit cell which can be straightforwardly, although technologically challengingly, extended to an one-dimensional array. Such an array would represent a medium with large Kerr constant. Moreover, this constant can be tuned over a wide range, even from positive to negative values. Although the sign of K is not important for an intermodulation gain which depends on K^2,[20] the sign of the Kerr constant can play an important role. For example, a tunable nonlinear medium can be used for wave-packet rectification and its properties depend on the sign of the Kerr constant.[23]

Moreover, such a material can mimic the behavior of a nematic optical media where the Kerr constant can change its sign.[24]

To demonstrate these features, we fabricated two ferromagnetically coupled qubits embedded in a coplanar waveguide resonator. The niobium resonator was fabricated by e-beam lithography and dry etching a 200 nm thick film on a silicon substrate. The aluminium qubit structures are placed in the middle of the resonator and were prepared by the shadow evaporation technique (Figure 1). Each qubit loop contains six Josephson junctions. In each qubit, one junction, with critical current I_{cqr}, is integrated within the centerline of the resonator. The bandwidth of our tunable parametric amplifier is $\approx$2 MHz. However, the unit cell of two qubits can be extended to an array, forming a metamaterial in a coplanar waveguide (see Figure 1). Thus, the enhanced interaction of the microwaves with one unit cell caused by the multiple reflections of the microwave signal at the coupling capacitors of the resonator can be substituted by the interaction of travelling waves with a large number of cells. By making use of such a microwave waveguide instead of a resonator the bandwidth can be increased considerably[17] and because of the high Kerr constant of qubits, it could operate as a wideband travelling wave parametric amplifier with large gain. Preparation of such quantum metamaterial is a technologically challenging task but we can investigate properties of the metamaterial in the standing waves configuration. Even in this configuration the bandwidth of our parametric amplifier is comparable with the bandwidth of parametric amplifiers used for cavity quantum electrodynamics experiments with superconducting qubits.[14,16] Such bandwidth is sufficient since the one of the superconducting cavities is narrower than 2 MHz.

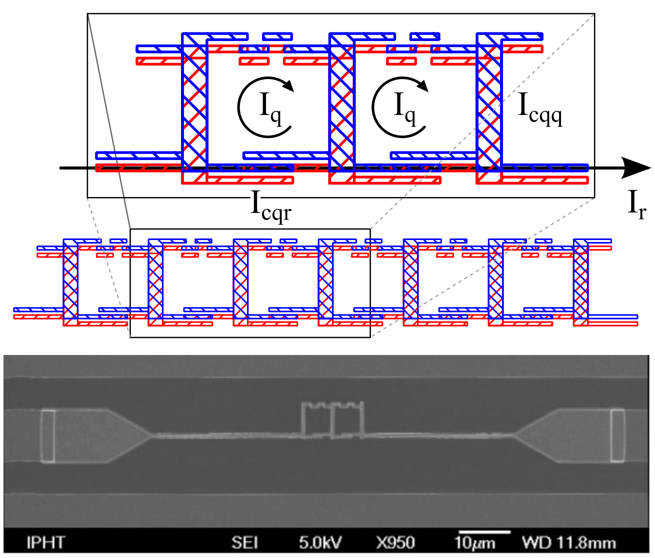

FIG. 1. Design of a unit cell which consists of two coupled qubits and its proposed (not implemented in this work) extension to an array of qubits (upper part). The bottom and upper electrodes are fabricated by shadow evaporation technique and marked by different hatching. The Josephson junctions are formed in areas where the hatchings overlap. The qubits share a large Josephson junction providing ferromagnetic coupling. Each qubit is strongly coupled to the resonator by a Josephson junction. The scanning electron microscope image of the sample (lower part) shows the unit cell of two qubits in the middle part of the resonator.

The qubits in the array are coupled by a shared large Josephson junction with a critical current I_{cqq}. The coupling energy between adjacent qubits is[25]

$$J_{qq} = \frac{\Phi_0 I_{qi-1} I_{qi}}{I_{cqq}}, \tag{4}$$

where I_{qi} is the persistent current of the ith qubit, I_{cqq} is the critical current of the coupling Josephson junction shared by adjacent qubits, and Φ_0 is the magnetic flux quantum. In the ground state, the persistent currents in adjacent qubits flow through the coupling Josephson junction in the same direction in order to minimize the total energy of the two coupled qubits. By proper design one can use the shadow evaporation technique to twist the electrodes of the coupling Josephson junction in such a way that ferromagnetic coupling is achieved (see Figure 1). For one qubit centered in a $\lambda/2$ resonator, the nonlinear inductance per unit length can be calculated from the relation[26]

$$\tilde{L} = \frac{F}{4\pi^2}\frac{\Phi_0^2}{\Delta}\frac{I_q^2}{I_{cqr}^2}\delta\left(x - \frac{l}{2}\right), \tag{5}$$

where $\delta(x)$ is the delta function, Δ and I_q are the tunneling amplitude and the persistent current of the superconducting flux qubit, respectively, and the function F is defined as

$$F = \frac{1}{\pi}\int_0^{2\pi} d\phi \frac{\cos^2\phi}{[1 + \eta^2(f_x + \gamma\sin\phi)^2]^{3/2}}, \tag{6}$$

where $\gamma = \Phi_0 I_q I_r/(2\pi I_{cqr}\Delta)$ and $\eta = \Phi_0 I_q/\Delta$. The coefficient $\tilde{L}_2$ is obtained from the Taylor expansion of the nonlinear inductance $\tilde{L}$.

Interactions with the measurement apparatus and the dissipative environment are modeled by making use of the test and the dissipative ports (details see in Ref. 20 and references therein). Parametric amplification is achieved by strong pumping of the resonator at a frequency $\omega_p/2\pi$. The pump frequency is mixed with a weak signal with frequency $\omega_s/2\pi$ by the nonlinear element, producing additional signals with angular frequencies ω_s and $2\omega_p - \omega_s$ (idler signal). In other words, two photons from the pump with angular frequency ω_p transform into two photons with angular frequencies ω_s and $2\omega_p - \omega_s$, while the energy is conserved. For strong pumping and in absence of fluctuations, the system can be described by the classical variables $\alpha = \langle a\rangle$, $\alpha^* = \langle a^\dagger\rangle$ and the average number of photons in the resonator[20] $\bar{n} = \alpha\alpha^*$

$$\bar{n}^3 + \frac{2(\omega_0 - \omega_p)K_n + 2\gamma\gamma_3}{K_n^2 + \gamma_3^2}\bar{n}^2 + \frac{(\omega_0 - \omega_p)^2 + \gamma^2}{K_n^2 + \gamma_3^2}\bar{n} = \frac{2\gamma_1^2}{K_n^2 + \gamma_3^2}\bar{n}_{in}, \tag{7}$$

where $\bar{n}_{in}$ is the average number of photons coming to the resonator from the input port in a time interval $1/\gamma_1$. The amplitude of the transmission coefficient of the resonator is given by the ratio $|t| = \bar{n}/\bar{n}_{in}$ and can be measured directly by a network analyzer.

Measurements were performed in a dilution refrigerator with a base temperature of 10 mK, where a biasing coil was

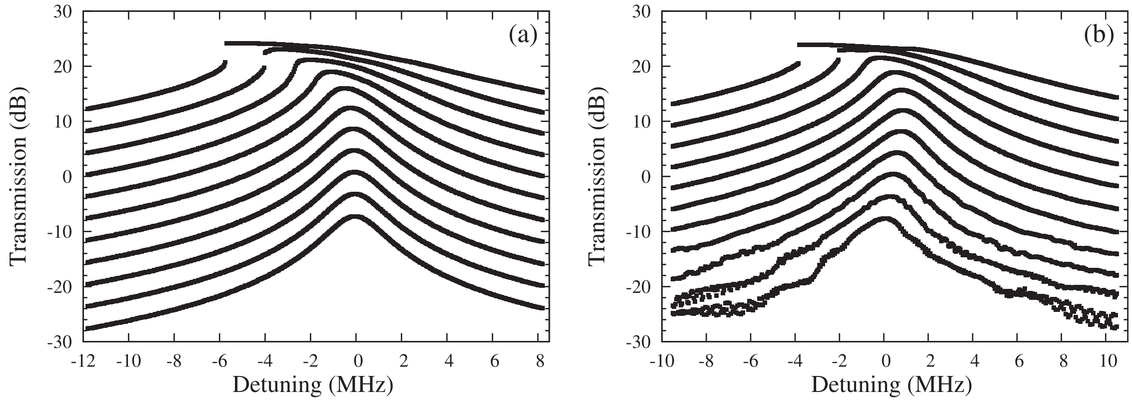

FIG. 2. Transmission of the resonator measured around the third harmonic (7.45 GHz) for an applied magnetic flux of $\Phi = 0$ (a) and $\Phi = \Phi_0/2$ (b). Curves, from bottom to top, correspond to an input power from -90 to -46 dBm increasing in 4 dBm steps. The curves are shifted by an increment of 4 dB along the y-axis for better visibility.

integrated into the sample holder to apply magnetic flux. First, the resonator was characterized by measuring its transmission and varying the input power and frequency (Figure 2). The resonance curve exhibits typical behavior of a Duffing oscillator.[27] From the low input power spectra, the resonance frequency of the third harmonic and its loaded quality factor were extracted: $f_3 = 7.45$ GHz and $Q = 3300$. The quality factor is determined by coupling capacitors of the resonator (internal quality factor is much higher than the external one) and it is in good agreement with microwave solver simulations. From the theoretical model,[20] we have calculated the ratio between the Kerr constant and the nonlinear dissipation $|K|/\gamma_3 \approx 3.5$ which satisfies the condition for an existence of a bistable region, $|K|/\gamma_3 > \sqrt{3}$. This kind of analysis is not possible for $\Phi = \Phi_0/2$, because as seen in Figure 3, for low input powers the transmission curve is bent towards the higher frequencies and with increasing power, the curve bends towards lower frequencies. This behavior can be modeled by a current (power) dependent Kerr constant

$$K_n = K_n^{(1)} + K_n^{(2)} \frac{I_r^2}{I_{cqr}^2}, \tag{8}$$

where $K_n^{(2)}$ corresponds to the fourth order term in the Taylor series given by Eq. (2). From qubit spectroscopy, we obtained the parameters that allow us to determine $\tilde{L}$ and subsequently $K_3^{(1)} = 3 \times 10^{-3}$ and $K_3^{(2)} = -6 \times 10^{-1}$. We investigated the detuning of the resonance frequency at different values of the applied magnetic field (Figure 3). We chose two working points: magnetic flux $\Phi = 0$, where the energy gap between the qubit's energy levels is large, and $\Phi = \Phi_0/2$, which corresponds to the qubits degeneracy point with an energy gap equal to the tunnelling amplitude Δ. The detuning of the resonance frequency of the resonator is inversely proportional to the energy gap[2,28] and is maximal at $\Phi = \Phi_0/2$.

The gain of the parametric amplifier was investigated in the following way: the transmission was measured at the signal frequency, while keeping its amplitude constant. The amplitude of the pump was greater than the amplitude of the signal, while simultaneously sweeping the amplitude and frequency of the pump. The frequency difference between the signal and the pump was 10 kHz (approximately 1% of the bandwidth of our resonator). The gain of the parametric amplifier depends on the frequency and the power of the pump (Figure 4). The magnetic flux applied to the qubits only slightly alters the resulting gain of both the signal and the idler, while the maximal gain is $\approx$20 dB. The main difference between these two cases is the presence of two high amplification branches at $\Phi = \Phi_0/2$ instead of only one present at $\Phi = 0$ and a periodic pattern of the gain depending on the bias flux (see Figure 4). These peculiarities may be a consequence of the quantum nature of the superconducting qubit (Landau–Zener beam splitting at the qubit degeneracy point[29]) and/or the modulation instability characteristic for wave propagation in a nonlinear dispersive media.[30,31] The modulation instability has recently been investigated in optical metamaterials taking into account both cubic and quintic nonlinearities.[32] It has been predicted that a combined effect of cubic-quintic nonlinearity increases the modulation instability gain. Our experimental results show that the quintic nonlinearity, which is characterized by a higher order Kerr constant $K_n^{(2)}$, cannot be neglected for strongly coupled superconducting qubits. Moreover, the shape of the idler gain is remarkably similar to the modulation instability gain shown in Refs. 31 and 32. A more detailed theoretical quantum analysis of parametric amplification is required in order to clarify this effect.

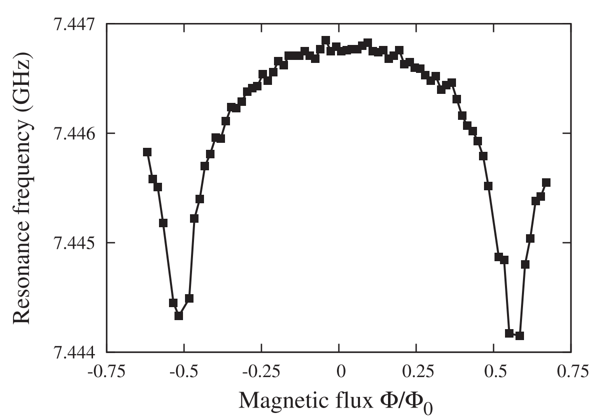

FIG. 3. Detuning of the resonance frequency of the resonator as a function of applied magnetic flux.

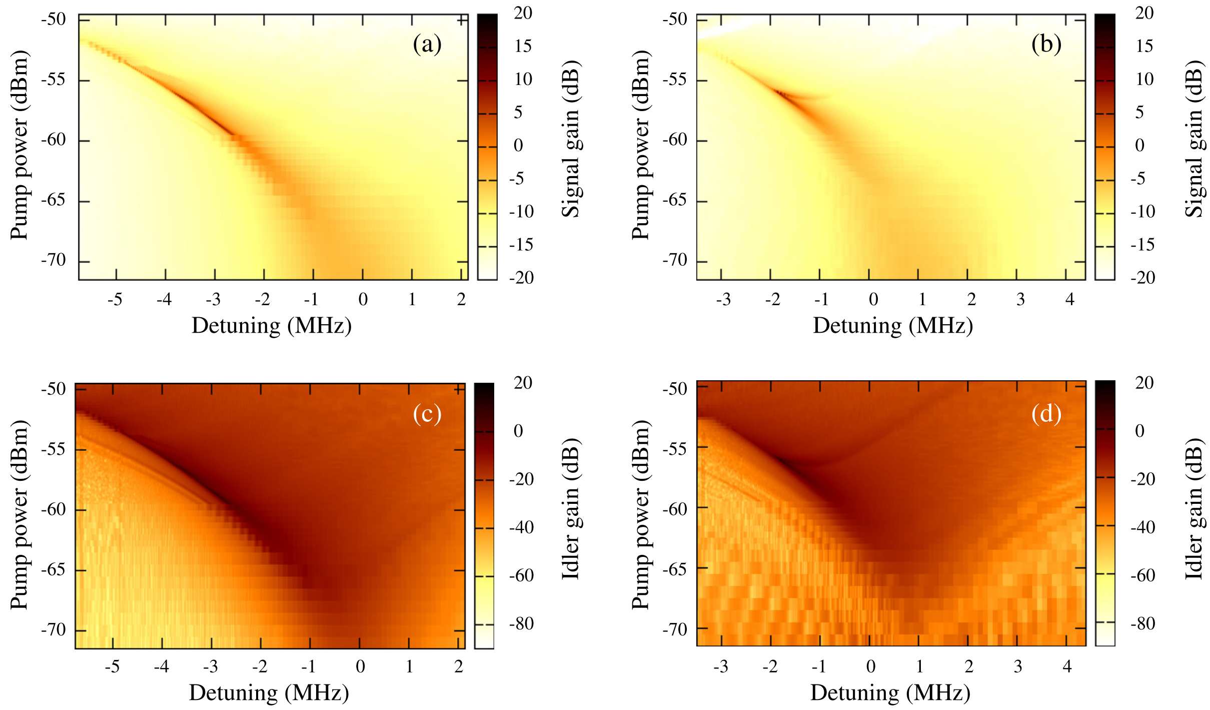

FIG. 4. Gain of the parametric amplifier as a function of detuning from the resonance frequency (x-axis) and the input pump power (y-axis). (a) Signal gain at a magnetic flux $\Phi = 0$ and (b) $\Phi = \Phi_0/2$. (c) Idler gain at $\Phi = 0$ and (d) $\Phi = \Phi_0/2$. The gain [dB] is defined as the difference between the signal or idler power [dBm] at the output of the resonator and the signal power [dBm] at the resonator input.

TABLE I. Comparison of superconducting parametric amplifiers.

$K^{(1)}/\omega_0$	$K^{(2)}/\omega_0$	Maximum gain (dB)	Lin. bandwidth (MHz)	References
-1.1×10^{-6}	…	30	17.5	33
-1.3×10^{-9}	…	22	2	34
-1.5×10^{-5}	…	28	2	35
$+3.0 \times 10^{-3}$	-6×10^{-1}	20	2	This paper

A noise temperature characterization of the parametric amplifier was not performed. However, our nonhysteretic device gives small contribution to the device noise corresponding to its effective temperature.[7] The effective temperature of the qubit was determined from independent measurement to be $T_{eff} \approx 100$ mK. Both gain and dynamic range of the parametric amplifier are higher than 20 dB which is enough to amplify its input noise above the noise level of HEMT amplifiers with noise temperature ~1 K.

In summary, we designed a parametric amplifier based on a superconducting coplanar waveguide resonator with a pair of integrated qubits serving as the nonlinear element. In contrast to other publications (see Table I), the Kerr constant of our system is *sign*-tunable and several orders of magnitude higher. Our amplifier achieves a maximal gain of 20 dB, which is comparable to the gain of similar superconducting parametric amplifiers.[14,16,17] The experiments reveal also two unknown features, namely, two branches of high amplification of the idler signal and in the case of a bias flux of $\Phi = \Phi_0/2$ a periodical pattern of the gain dependent on the flux itself.

The research leading to these results has received funding from the European Community's Seventh Framework Programme (FP7/2007-2013) under Grant No. 270843 (iQIT) and DO7RP-0032-11. This work was also supported by the Slovak Research and Development Agency under the Contract APVV-0515-10 (former Project Nos. VVCE-0058-07 and APVV-0432-07) and LPP-0159-09. The authors gratefully acknowledge the financial support of the EU through the ERDF OP R&D, Project CE QUTE & metaQUTE.

[1] J. Q. You and F. Nori, Phys. Rev. B **68**, 064509 (2003).
[2] M. Grajcar, A. Izmalkov, and E. Il'ichev, Phys. Rev. B **71**, 144501 (2005).
[3] Z.-L. Xiang, S. Ashhab, J. Q. You, and F. Nori, Rev. Mod. Phys. **85**, 623 (2013).
[4] M. D. Reed, L. DiCarlo, S. E. Nigg, L. Sun, L. Frunzio, S. M. Girvin, and R. J. Schoelkopf, Nature **482**, 382–385 (2012).
[5] A. Fedorov, L. Steffen, M. Baur, M. P. da Silva, and A. Wallraff, Nature **481**, 170–172 (2012).
[6] N. Oukhanski, M. Grajcar, E. Il'ichev, and H.-G. Meyer, Rev. Sci. Instrum. **74**, 1145 (2003).
[7] L. S. Kuzmin, K. K. Likharev, V. V. Migulin, and A. B. Zorin, IEEE Trans. Magn. **19**, 618 (1983).
[8] A. M. Zagoskin, E. Il'ichev, M. W. McCutcheon, J. F. Young, and F. Nori, Phys. Rev. Lett. **101**, 253602 (2008).
[9] M. A. Castellanos-Beltran, K. D. Irwin, G. C. Hilton, L. R. Vale, and K. W. Lehnert, Nat. Phys. **4**, 929 (2008).
[10] T. Yamamoto, K. Inomata, M. Watanabe, K. Matsuba, T. Miyazaki, W. D. Oliver, Y. Nakamura, and J. S. Tsai, Appl. Phys. Lett. **93**, 042510 (2008).
[11] F. Mallet, M. A. Castellanos-Beltran, H. S. Ku, S. Glancy, E. Knill, K. D. Irwin, G. C. Hilton, L. R. Vale, and K. W. Lehnert, Phys. Rev. Lett. **106**, 220502 (2011).
[12] N. Bergeal, F. Schackhert, M. Metcalfe, R. Vijay, V. E. Manucharyan, L. Frunzio, D. E. Prober, R. J. Schoelkopf, S. M. Girvin, and M. H. Devoret, Nature **465**, 64 (2010).
[13] M. Hatridge, R. Vijay, D. H. Slichter, J. Clarke, and I. Siddiqi, Phys. Rev. B **83**, 134501 (2011).
[14] B. Abdo, O. Suchoi, E. Segev, O. Shtempluck, M. Blencowe, and E. Buks, Europhys. Lett. **85**, 68001 (2009).
[15] K. M. Sundqvist, S. Kintas, M. Simoen, P. Krantz, M. Sandberg, C. M. Wilson, and P. Delsing, Appl. Phys. Lett. **103**, 102603 (2013).
[16] E. A. Tholén, A. Ergül, E. M. Doherty, F. M. Weber, F. Grégis, and D. B. Haviland, Appl. Phys. Lett. **90**, 253509 (2007).

[17]B. Ho Eom, P. K. Day, H. G. LeDuc, and J. Zmuidzinas, Nat. Phys. **8**, 623 (2012).
[18]E. Il'ichev and Y. S. Greenberg, Europhys. Lett. **77**, 58005 (2007).
[19]S. Savel'ev, A. M. Zagoskin, A. L. Rakhmanov, A. N. Omelyanchouk, Z. Washington, and F. Nori, Phys. Rev. A **85**, 013811 (2012).
[20]B. Yurke and E. Buks, J. Lightwave Technol. **24**, 5054 (2006).
[21]M. Grajcar, A. Izmalkov, S. H. W. van der Ploeg, S. Linzen, T. Plecenik, T. Wagner, U. Hübner, E. Il'ichev, H.-G. Meyer, A. Y. Smirnov *et al.*, Phys. Rev. Lett. **96**, 047006 (2006).
[22]A. Y. Smirnov, "Signature of entangled eigenstates in the magnetic response of two coupled flux qubits," e-print arXiv:cond-mat/0312635.
[23]Y. Li, J. Zhou, F. Marchesoni, and B. Li, Sci. Rep. **4**, 4566 (2014).
[24]L. M. Blinov and V. G. Blinov, *Electrooptic Effects in Liquid Crystal Materials* (Springer-Verlag, New York, Inc., 1994).
[25]M. Grajcar, A. Izmalkov, S. H. W. van der Ploeg, S. Linzen, E. Il'ichev, T. Wagner, U. Hübner, H.-G. Meyer, A. Maassen van den Brink, S. Uchaikin *et al.*, Phys. Rev. B **72**, 020503 (2005).
[26]Y. S. Greenberg, A. Izmalkov, M. Grajcar, E. Il'ichev, W. Krech, H.-G. Meyer, M. H. S. Amin, and A. M. van den Brink, Phys. Rev. B **66**, 214525 (2002).
[27]I. Kovacic and M. J. Brennan, *The Duffing Equation. Nonlinear Oscillators and their Behaviour* (John Wiley & Sons Ltd., 2011).
[28]A. N. Omelyanchouk, S. N. Shevchenko, Y. S. Greenberg, O. Astafiev, and E. Il'ichev, Low Temp. Phys. **36**, 893 (2010).
[29]S. N. Shevchenko, S. H. W. van der Ploeg, M. Grajcar, E. Il'ichev, A. N. Omelyanchouk, and H.-G. Meyer, Phys. Rev. B **78**, 174527 (2008).
[30]A. Ostrovskii, Zh. Eksp. Teor. Fiz **51**, 1189 (1966) [Sov. Phys. JETP. **24**, 797 (1966)] http://www.jetp.ac.ru/cgi-bin/e/index/e/24/4/p797?a=list.
[31]G. P. Agrawal, Phys. Rev. Lett. **59**, 880 (1987).
[32]M. Saha and A. K. Sarma, Opt. Commun. **291**, 321 (2013).
[33]C. Eichler, D. Bozyigit, C. Lang, M. Baur, L. Steffen, J. M. Fink, S. Filipp, and A. Wallraff, Phys. Rev. Lett. **107**, 113601 (2011).
[34]E. A. Tholén, A. Erguel, K. Stannigel, C. Hutter, and D. B. Haviland, Phys. Scr. **2009**, 014019.
[35]M. A. C. Beltran and K. W. Lehnert, Appl. Phys. Lett. **91**, 083509 (2007).